

# A divergence-free finite element method for a type of 3D Maxwell equations

Dedicated to Professor George C. Hsiao on the occasion of his 75th birthday

Jianguo Huang<sup>a,1</sup>, Shangyou Zhang<sup>b,\*</sup>

<sup>a</sup>*Department of Mathematics, Shanghai Jiao Tong University, Shanghai 200240;  
Division of Computational Science, E-Institute of Shanghai Universities, Shanghai  
Normal University, China*

<sup>b</sup>*Department of Mathematical Sciences, University of Delaware, Newark, DE 19716*

---

## Abstract

We seek a divergence-free finite element solution for the magnetic field governed by the static Maxwell equations. As usual, the solution is represented as a curl of a vector potential. Typically, this vector potential is uniquely defined in a divergence-free space. The novelty of our method is that we use some simple but non divergence-free finite element spaces. In this way, the finite element vector potential does not approximate the divergence-free vector, but its curl is divergence-free and is exactly the same solution obtained by the divergence-free finite element potential. Computationally, the finite element solution for the magnetic field is obtained directly as a certain weighted  $L^2$ -orthogonal projection within the divergence-free finite element subspace. Optimal order convergence is shown for the method. Numerical tests are provided.

*Keywords:* Maxwell equations, vector potential, divergence-free element, rectangular grids.

*2000 MSC:* 65M60, 65N30, 76M10, 76D07

---

\*Corresponding author

*Email addresses:* [jghuang@sjtu.edu.cn](mailto:jghuang@sjtu.edu.cn) (Jianguo Huang), [szhang@udel.edu](mailto:szhang@udel.edu) (Shangyou Zhang)

<sup>1</sup>The work of this author was partly supported by the NNSFC (10771138) and E-Institutes of Shanghai Municipal Education Commission (E03004).

## 1. Introduction

We deal with the problem of numerically solving the magnetic field  $\mathbf{B}$  (or equivalently  $\mathbf{H}$ ), governed by the static Maxwell equations:

$$\begin{cases} \nabla \times \mathbf{H} = \mathbf{J} & \text{in } \Omega, \\ \nabla \cdot \mathbf{B} = 0 & \text{in } \Omega, \\ \mathbf{B} = \mu(\mathbf{x})\mathbf{H} & \text{in } \Omega, \\ \mathbf{n} \cdot \mathbf{B} = 0 & \text{on } \partial\Omega, \end{cases} \quad (1.1)$$

where  $\Omega \subset \mathbf{R}^3$  is a bounded and simply connected domain with the Lipschitz boundary  $\partial\Omega$ ,  $\mathbf{n}$  is the unit outward normal on  $\partial\Omega$ ,  $\mu(\mathbf{x})$  is the material susceptibility, and  $\mathbf{J}(\mathbf{x})$  is the current density satisfying  $\nabla \cdot \mathbf{J} = 0$ .

The equations (1.1) are a div-curl system, and similar systems also occur in the field of fluid dynamics. In the past three decades, several numerical methods have been developed for such kind of problems, e.g., the finite element method [11, 13], the covolume method [17], the discontinuous least squares method [2], the locally divergence-free discontinuous Galerkin method [5] and some novel methods [3]. Since the magnetic field  $\mathbf{B}$  is divergence free, as used in computational fluid dynamics [6], it is common to reformulate (1.1) in potential formulations [11, 13, 21]. For this, we introduce a vector potential  $\mathbf{u}$  for  $\mathbf{B}$  (cf. [1, 7, 14]) such that

$$\mathbf{B} = \nabla \times \mathbf{u} \quad \text{in } \Omega, \quad (1.2)$$

$$\nabla \cdot \mathbf{u} = 0 \quad \text{in } \Omega, \quad (1.3)$$

$$\mathbf{n} \times \mathbf{u} = \mathbf{0} \quad \text{on } \partial\Omega. \quad (1.4)$$

Then, using the relation  $\mathbf{H} = \mu^{-1}(\mathbf{x})\mathbf{B}$  and the equalities (1.2) and (1.4), we can write the first equation in (1.1) as  $\nabla \times (\mu^{-1}(\mathbf{x})\nabla \times \mathbf{u}) = \mathbf{J}$ . By Green's formula for vector fields and assuming  $\mathbf{B} \in H^1(\Omega)^3$ , the weak formulation for  $\mathbf{u}$  reads

$$(\mu^{-1}(\mathbf{x})\nabla \times \mathbf{u}, \nabla \times \mathbf{v})_{L^2(\Omega)^3} = (\mathbf{J}, \mathbf{v})_{L^2(\Omega)^3}, \quad \mathbf{u}, \mathbf{v} \in \mathbf{H}_t^1(\text{curl}), \quad (1.5)$$

where the Sobolev space  $\mathbf{H}_t^1(\text{curl})$  is defined by

$$\mathbf{H}_t^1(\text{curl}) = \{\mathbf{v} \in H^1(\Omega)^3 \mid \nabla \times \mathbf{v} \in H^1(\Omega)^3, \mathbf{n} \times \mathbf{u} = \mathbf{0} \text{ on } \partial\Omega\}. \quad (1.6)$$

It is difficult to solve finite element equations discretizing (1.5), for two reasons. The bilinear form in (1.5) is not positive definite and there is an additional constraint (1.3) for the problem (1.5). An effective method

was proposed in [14] that a discrete div-div form is added to (1.5) for an edge-element method of [16]. The resulting positive definite problem is then solved by the multigrid method in the optimal order of computation [14].

In this work, we propose a different method, based on the divergence-free finite element on rectangular grids in 3D. First the weak problem (1.5), when  $\mathbf{B}$  (or  $\mathbf{H}$ ) is needed only, is equivalent to

$$(\mu^{-1}(\mathbf{x})\mathbf{B}, \mathbf{w})_{L^2(\Omega)^3} = (\mathbf{J}, \mathbf{v})_{L^2(\Omega)^3}, \quad \mathbf{B} \in \mathbf{Z}_{\mathbf{n}} \text{ and for all } \mathbf{v} \in \mathbf{H}_t^1(\text{curl}), \quad (1.7)$$

where  $\mathbf{w} = \nabla \times \mathbf{v}$  and  $\mathbf{Z}_{\mathbf{n}}$  is a divergence-free space, defined by

$$\mathbf{Z}_{\mathbf{n}} = \{ \mathbf{v} \in H^1(\Omega)^3 \mid \nabla \cdot \mathbf{v} = 0 \text{ in } \Omega, \mathbf{n} \cdot \mathbf{v} = 0 \text{ on } \partial\Omega \}. \quad (1.8)$$

Thus, we seek the divergence-free finite element solution  $\mathbf{B}_h$  for  $\mathbf{B}$  directly, without computing the potential  $\mathbf{u}_h$ . To do so, we construct a corresponding subspace  $\mathbf{S}_h^k$  of  $\mathbf{H}_t^1(\text{curl})$  (cf. (3.17) below) so that the corresponding finite element equations for (1.5) becomes

$$(\mu^{-1}(\mathbf{x})\mathbf{B}_h, \mathbf{w}_h) = (\mathbf{J}, \mathbf{v}_h), \quad \mathbf{B}_h \in \mathbf{Z}_h^k \text{ and for all } \mathbf{v}_h \in \mathbf{S}_h^k, \quad (1.9)$$

where  $\mathbf{w}_h = \nabla \times \mathbf{v}_h$ , is in the divergence-free finite element space  $\mathbf{Z}_h^k$  defined by (2.7). Here  $\mathbf{v}_h$  is not unique, for a given  $\mathbf{w}_h$ . But  $\mathbf{B}_h$  is the unique weighted  $L^2$ -orthogonal projection of  $\mathbf{B}$  in the **previous finite element space**  $\mathbf{Z}_h^k$ .

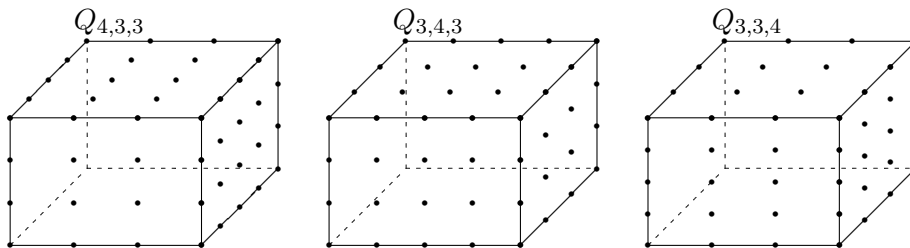


Figure 1: The  $\mathbf{V}_h^k$  finite element (2.6),  $k = 3$ . (Showing face nodes.)

The advantage of the new method (1.9) is that we completely ignore the divergence-free constraint (1.3) on the vector potential  $\mathbf{u}$ . We do not need to compute the finite element vector-potential. Of course, if we do

compute such a finite element potential, it is not of much use as it does not approximate the potential  $\mathbf{u}$  of (1.5) at all. A similar idea was used in [6, 18] where a discrete axial gauge condition is applied to eliminate some degrees of freedom for the finite element. The finite element potential does not approximate  $\mathbf{u}$  either, but its curl does approximate  $\nabla \times \mathbf{u} = \mathbf{B}$ . **The approach in [6]** is based on a graph analysis of grids, while **our work here is directed to** finding all divergence-free elements and a set of their (non divergence-free) vector potentials. **Though** the method is simpler, it is limited to rectangular grids in 2D and 3D, for example, an L-shaped domain equipped with a rectangular grid, at the moment. **However**, the method could be extended to other divergence-free finite elements. For example, on general triangular grids, by choosing the Morgan-Scott complete  $C^1$ - $P_{k+1}$  basis [15] as our potential basis, our method would produce a finite element solution  $\mathbf{B}_h$  for (1.9) in the  $P_k$  divergence-free finite element space ( $k \geq 4$ , cf. [19]). In principle, the method can be applied to any divergence-free finite element method if we are willing to find a basis for the potential space. But the method is no longer as simple as it is on regular grids.

The new method is also limited to continuous permeability  $\mu(\mathbf{x})$  in (1.1). Or it is applicable in combination with the domain decomposition method when  $\mu(\mathbf{x})$  is continuous within each subdomain. When  $\mu(\mathbf{x})$  is piecewise continuous, the continuity/regularity of  $\mathbf{B}$  is not fully known, cf. [10] and references therein. Similar to our method, there are other continuous finite element methods for the Maxwell equations (1.1), for example, in [12]. To be precise, the divergence-free finite element here is a continuous, piecewise polynomials of different degrees in different direction, shown in Figure 1. Such finite elements are designed and studied in [24] and [25].

## 2. The finite element discretization and convergence

We consider the static Maxwell equations (1.1). It is assumed the system (1.1) is consistent in that

$$\nabla \cdot \mathbf{J} = 0 \quad \text{in } \Omega.$$

We further assume the domain  $\Omega$ , the coefficient  $\mu(\mathbf{x})$  and the data  $\mathbf{J}$  are smooth enough so that a regularity of  $H^1$  or better for the solution (1.1) holds,

$$\mathbf{B} \in H^r(\Omega)^3 \cap \mathbf{H}_n(\text{curl}) \quad \text{for some } r \geq 1, \quad (2.1)$$

where

$$\mathbf{H}_n(\text{curl}) = \{ \mathbf{v} \in L^2(\Omega)^3 \mid \nabla \times \mathbf{v} \in L^2(\Omega)^3, \mathbf{n} \cdot \mathbf{v} = 0 \text{ on } \partial\Omega \}.$$

For a vector field  $\mathbf{B}$ , let  $\mathbf{u}$  be a vector field determined by (1.2)-(1.4). By the regularity assumption (2.1), the weak formulation of the potential problem is (1.5), i.e.,

$$\begin{aligned} (\mu^{-1}(\mathbf{x})\nabla \times \mathbf{u}, \nabla \times \mathbf{v})_{L^2(\Omega)^3} &= (\mathbf{J}, \mathbf{v})_{L^2(\Omega)^3}, \\ \mathbf{u} &\in \mathbf{H}_t^1(\text{curl}) \quad \text{and for all } \mathbf{v} \in \mathbf{H}_t^1(\text{curl}). \end{aligned} \quad (2.2)$$

However, we have a constraint, i.e., the gauge condition, for the potential  $\mathbf{u}$ :

$$\nabla \cdot \mathbf{u} = 0 \quad \text{in } \Omega. \quad (2.3)$$

For simplicity, we assume that the potential solution  $\mathbf{u}$  of (2.2) and (2.3) has a lifting regularity if (2.1) is satisfied:

$$\|\mathbf{u}\|_{H^{r+1}(\Omega)^3} \leq C\|\mathbf{B}\|_{H^r(\Omega)^3}. \quad (2.4)$$

We remark that the assumptions (2.1) and (2.4) are given only for theoretical analysis. They are very strong but are really fulfilled when the domain  $\Omega$  and the susceptibility function  $\mu$  are smooth enough. In fact, if  $\partial\Omega \in C^{1,1}$  or  $\Omega$  is a convex polyhedron,  $\mathbf{J} \in L^2(\Omega)^3$ ,  $\mu \in C^1(\bar{\Omega})$  and there exist two positive constants  $C_0$  and  $C_1$  such that  $C_0 \leq \mu(\mathbf{x}) \leq C_1$  for all  $\mathbf{x} \in \bar{\Omega}$ , from Theorems 3.5 and 3.6 and Corollary 3.7 in [7] and a similar argument for deriving Theorem 5.2 in [10], we find that the solution  $\mathbf{B}$  of (1.1) lies in  $H^1(\Omega)^3$ , with the bound  $\|\mathbf{B}\|_{H^1(\Omega)^3} \leq C\|\mathbf{J}\|_{L^2(\Omega)^3}$ . Furthermore, if  $\partial\Omega \in C^{2,1}$ , for the vector potential  $\mathbf{u}$  determined by (1.2)-(1.4), we have from Corollaries 3.3 and 3.7 in [7] that  $\mathbf{u} \in H^2(\Omega)^3$ , with the bound  $\|\mathbf{u}\|_{H^2(\Omega)^3} \leq C\|\mathbf{B}\|_{H^1(\Omega)^3}$ .

In the new method to be proposed, we completely ignore the condition (2.3) when solving (2.2). The idea is to find any one solution of (1.5), in the finite element method. We only want the curl of such a finite element potential, but not the potential itself. That is, in the numerical method we propose, we seek an approximate solution for  $\mathbf{B}$  directly, instead of its vector potential  $\mathbf{u}$ . As described at (1.7), the original problem for  $\mathbf{B}$  can be characterized as: Find  $\mathbf{B} \in \mathbf{Z}_n$  such that

$$\begin{aligned} (\mu^{-1}(\mathbf{x})\mathbf{B}, \mathbf{w})_{L^2(\Omega)^3} &= (\mathbf{J}, \mathbf{v})_{L^2(\Omega)^3} \quad \text{for all } \mathbf{w} \in \mathbf{Z}_n \\ &\text{and for all } \mathbf{v} \in \mathbf{H}_t^1(\text{curl}), \end{aligned} \quad (2.5)$$

where  $\mathbf{w} = \nabla \times \mathbf{v}$ , and the spaces  $\mathbf{Z}_n$  and  $\mathbf{H}_t^1(\text{curl})$  are defined in (1.8) and (1.6), respectively. Please notice that the divergence-free constraint is omitted in the definition of  $\mathbf{H}_t^1(\text{curl})$ . It is interesting to know that, in (2.5),  $\mathbf{v}$  is itself a solution of the original Maxwell equations (1.1):

$$\begin{cases} \nabla \times \mathbf{v} = \mathbf{w} & \text{in } \Omega, \\ \nabla \cdot \mathbf{v} = 0 & \text{in } \Omega, \\ \mathbf{n} \cdot \mathbf{v} = 0 & \text{on } \partial\Omega. \end{cases}$$

But in the computation,  $\mathbf{v}$  are given as some basis functions in the potential space (without divergence-free constraint).

Next, we introduce a special finite element method for problem (1.1) based on the above formulation. Let the domain  $\Omega$  be subdivided into rectangular cubes, denoted as  $\mathcal{T}_h$ , where  $h$  stands for the maximal element size. The  $k$ -th order finite element space is defined by, cf. Figure 1, for all  $k \geq 2$ ,

$$\mathbf{V}_h^k = \left\{ \mathbf{v}_h = (v_1 \ v_2 \ v_3)^T \in C(\Omega)^3 \mid v_1|_K \in Q_{k+1,k,k}, \right. \\ \left. v_2|_K \in Q_{k,k+1,k}, v_3|_K \in Q_{k,k,k+1}, \forall K \in \mathcal{T}_h; \mathbf{n} \cdot \mathbf{v}_h|_{\partial\Omega} = 0 \right\}, \quad (2.6)$$

where the polynomial spaces are denoted by their separated degrees

$$Q_{i',j',k'} = \left\{ \sum_{i=0}^{i'} \sum_{j=0}^{j'} \sum_{k=0}^{k'} c_{ijk} x^i y^j z^k \right\}.$$

In (2.6), we require  $k \geq 2$ . A divergence-free piecewise polynomial function would be  $C^1$  in  $x$  direction for its first component  $v_1$ ,  $C^1$  in  $y$  direction for its second component  $v_2$  and  $C^1$  in  $z$  direction for its third component  $v_3$ . This can be seen as  $(v_1)_x = -(v_2)_y - (v_3)_z$  while the two functions on the right side are continuous in  $x$  direction. The minimal degree  $C^1$ -element is the cubic Bogner-Fox-Schmit element, i.e., the  $C^1$ - $Q_{3,3,3}$  element. This is why we do not allow  $k = 1$  in (2.6). The construction of a potential space for the divergence-free subspace of  $\mathbf{V}_h^k$  is based on the Bogner-Fox-Schmit element, or its higher order extension [25].

The divergence-free finite element spaces are defined by

$$\mathbf{Z}_h^k = \left\{ \mathbf{z}_h \in \mathbf{V}_h^k \mid \nabla \cdot \mathbf{z}_h = 0 \text{ in } \Omega \right\}. \quad (2.7)$$

The finite element approximation for (2.5) is: Find  $\mathbf{B}_h \in \mathbf{Z}_h^k$  such that

$$(\mu^{-1}(\mathbf{x})\mathbf{B}_h, \mathbf{w}_h) = (\mathbf{J}, \mathbf{v}_h) \quad \forall \mathbf{w}_h \in \mathbf{Z}_h^k, \quad (2.8)$$

where  $\mathbf{v}_h \in \mathbf{S}_h^k$ , defined below in (2.11) and (3.17), such that  $\nabla \times \mathbf{v}_h = \mathbf{w}_h$ . For simplicity, we drop the index  $L^2(\Omega)^3$  for the  $L^2$ -inner product in (2.8), and from here on. Traditionally, the potential  $\mathbf{v}_h$  in (2.8) is chosen uniquely in a **divergence-free?** space, i.e.,  $\nabla \cdot \mathbf{v}_h = 0$  and  $\nabla \times \mathbf{v}_h = \mathbf{w}_h$ . In our method, we relax the condition  $\nabla \cdot \mathbf{v}_h = 0$ . But it is still a challenge to find an “exact” potential finite element space  $\mathbf{S}_h^k$  for a finite element space  $\mathbf{V}_h^k$ , i.e., each  $\mathbf{w}_h \in \mathbf{Z}_h^k$  has a unique  $\mathbf{v}_h \in \mathbf{S}_h^k$  such that  $\nabla \times \mathbf{v}_h = \mathbf{w}_h$ . In other words, we need to find a space  $\mathbf{S}_h^k$  such that

$$\nabla \times \mathbf{S}_h^k = \mathbf{Z}_h^k \quad \text{and} \quad \{\mathbf{v}_h \in \mathbf{S}_h^k \mid \nabla \times \mathbf{v}_h = \mathbf{0}\} = \{\mathbf{0}\}. \quad (2.9)$$

Toward this purpose, we introduce a larger potential space:

$$\begin{aligned} \tilde{\mathbf{S}}_h^k = \left\{ \mathbf{s}_h = (s_1 \quad s_2 \quad s_3)^T \in C(\Omega)^3 \mid s_1|_K \in Q_{k,k+1,k+1}, \right. \\ \left. s_2|_K \in Q_{k+1,k,k+1}, s_3|_K \in Q_{k+1,k+1,k}, \forall K \in \mathcal{T}_h; \right. \\ \left. \nabla \times \mathbf{s}_h \in \mathbf{V}_h^k, \mathbf{n} \times \mathbf{s}_h|_{\partial\Omega} = \mathbf{0} \right\}. \end{aligned} \quad (2.10)$$

It is easy to verify that  $\{\nabla \times \mathbf{v}_h \mid \mathbf{v}_h \in \tilde{\mathbf{S}}_h^k\} \subset \mathbf{Z}_h^k$ . But we do not know if  $\tilde{\mathbf{S}}_h^k$  is a potential space for  $\mathbf{Z}_h^k$  yet, that is, if  $\nabla \times \tilde{\mathbf{S}}_h^k \supset \mathbf{Z}_h^k$ . Our goal is to find one (nonunique) subspace  $\mathbf{S}_h^k \subset \tilde{\mathbf{S}}_h^k$ , in (3.17) next section, satisfying (2.9), or equivalently satisfying (as  $\nabla \times \mathbf{S}_h^k \subset \mathbf{Z}_h^k$ )

$$\nabla \times \mathbf{S}_h^k = \mathbf{Z}_h^k \quad \text{and} \quad \dim \mathbf{S}_h^k = \dim \mathbf{Z}_h^k. \quad (2.11)$$

Therefore, a basis for  $\mathbf{S}_h^k$  forms a potential basis for  $\mathbf{Z}_h^k$ , under the curl operator. Again, because

$$\mathbf{Z}_h^k = \nabla \times \mathbf{S}_h^k \subset \nabla \times \tilde{\mathbf{S}}_h^k \subset \mathbf{Z}_h^k,$$

the larger space  $\tilde{\mathbf{S}}_h^k$  is also a potential space for  $\mathbf{Z}_h^k$ .

In particular, we have the following inclusions for the *conforming* finite element spaces, cf. (1.6) and (1.8),

$$\mathbf{S}_h^k \subset \tilde{\mathbf{S}}_h^k \subset \mathbf{H}_t^1(\text{curl}) \quad \text{and} \quad \mathbf{Z}_h^k \subset \mathbf{Z}_n.$$

The advantage of the new method is that we do not need to find a divergence-free basis for a subspace of the potential space  $\tilde{\mathbf{S}}_h^k$ . Nevertheless, it is still a tedious work to find one  $\mathbf{S}_h^k$  and one basis for it. Please note that the definitions of  $\mathbf{S}_h^k$  and  $\tilde{\mathbf{S}}_h^k$  are abstract in (2.9), (2.11) and (2.10). We will give them constructive definitions next section, after we find the dimension of  $\mathbf{Z}_h^k$ .

**Theorem 2.1.** *The finite element equation (2.8) has a unique solution  $\mathbf{B}_h \in \mathbf{Z}_h^k$ .*

**Proof .** As we have the weighted  $L^2$ -inner product as the bilinear form in the equation (2.8), it has a unique solution in any  $L^2$  space, in particular the space  $\mathbf{Z}_h^k$ . But we have to show that the right hand side is independent of the choice of  $\mathbf{v}_h$  used in (2.8). First, by (2.10), (2.9) and (2.11), it is apparent that

$$\left\{ \nabla \times \mathbf{s}_h \mid \mathbf{s}_h \in \tilde{\mathbf{S}}_h^k \right\} = \left\{ \nabla \times \mathbf{s}_h \mid \mathbf{s}_h \in \mathbf{S}_h^k \right\} = \mathbf{Z}_h^k. \quad (2.12)$$

In fact, this is to be proved in Proposition 3.1 in the next section, as we have abstract definitions here, i.e., not showing the existence of  $\mathbf{S}_h^k$  yet. By (2.12), let  $\mathbf{v}_1$  be one (unique) such function in  $\mathbf{S}_h^k$  and  $\mathbf{v}_2$  be another one in  $\tilde{\mathbf{S}}_h^k$  such that  $\nabla \times \mathbf{v}_1 = \mathbf{w}_h = \nabla \times \mathbf{v}_2$ . Then the right hand side of (2.8) is independent of the choice of  $\mathbf{v}_i$ :

$$\begin{aligned} (\mathbf{J}, \mathbf{v}_2) &= (\mathbf{J}, \mathbf{v}_2 - \mathbf{v}_1) + (\mathbf{J}, \mathbf{v}_1) = (\nabla \times \mathbf{H}, \mathbf{v}_2 - \mathbf{v}_1) + (\mathbf{J}, \mathbf{v}_1) \\ &= (\mathbf{H}, \nabla \times (\mathbf{v}_2 - \mathbf{v}_1)) + (\mathbf{J}, \mathbf{v}_1) = (\mathbf{J}, \mathbf{v}_1). \end{aligned}$$

The theorem is proved. ■

As we define  $\mathbf{Z}_h = \nabla \times \tilde{\mathbf{S}}_h^k$ , the approximation property of  $\mathbf{Z}_h$  is inherited from that of  $\tilde{\mathbf{S}}_h^k$ , the space of  $C^1$ - $Q_{k+1}$  functions. In particular, the nodal value interpolation operator  $\mathbf{I}_h$  on  $\tilde{\mathbf{S}}_h^k$  is stable for smoothing functions and provides an optimal order approximator  $\mathbf{I}_h \mathbf{u}$  to  $\mathbf{u}$ . This way, we would get implicitly an interpolation operator (nonlocal) on the space  $\mathbf{Z}$  to  $\mathbf{Z}_h$ :  $(\nabla \times \mathbf{I}_h) \circ (\nabla \times)^{-1}$  where  $(\nabla \times)^{-1}$  is the inverse operator defined by the solution of (1.5). Via it, we obtain the best order approximation for the solution  $\mathbf{B}_h$  without constructing such a  $\mathbf{w}_h$  in the subspace  $\mathbf{Z}_h$ , differently from the standard procedure. It is possible but difficult to construct a local interpolation operator preserving the divergence from  $\mathbf{Z}$  to  $\mathbf{Z}_h$ , cf. [9, 23] for a few such operators.

**Theorem 2.2.** *The finite element solution  $\mathbf{B}_h$ , defined in (2.8), approximates the solution  $\mathbf{B}$  of (2.5) in the optimal order:*

$$\|\mathbf{B} - \mathbf{B}_h\|_{L^2(\Omega)^3} \leq Ch^{\min\{k,r\}} \|\mathbf{B}\|_{H^r(\Omega)^3}, \quad (2.13)$$

*assuming the regularity conditions (2.1) and (2.4) hold.*

**Proof .** This is a standard C ea's lemma [4]. Subtracting (2.8) from (2.5), we get the typical orthogonal projection:

$$(\mu^{-1}(x)(\mathbf{B} - \mathbf{B}_h), \mathbf{w}_h) = 0 \quad \forall \mathbf{w}_h \in \mathbf{Z}_h^k.$$

This, together with the condition:  $C_0 \leq \mu(\mathbf{x}) \leq C_1$  for all  $\mathbf{x} \in \bar{\Omega}$ , implies that, for all  $\mathbf{w}_h \in \mathbf{Z}_h^k$ ,

$$\begin{aligned} C_1^{-1} \|\mathbf{B} - \mathbf{B}_h\|_{L^2(\Omega)^3}^2 &\leq (\mu^{-1}(x)(\mathbf{B} - \mathbf{B}_h), \mathbf{B} - \mathbf{B}_h) \\ &= (\mu^{-1}(x)(\mathbf{B} - \mathbf{B}_h), \mathbf{B} - \mathbf{w}_h) \\ &\leq C_0^{-1} \|\mathbf{B} - \mathbf{B}_h\|_{L^2(\Omega)^3} \|\mathbf{B} - \mathbf{w}_h\|_{L^2(\Omega)^3}. \end{aligned} \quad (2.14)$$

Next, let the potential  $\mathbf{u}$  be defined in (1.5). Let  $\mathbf{I}_h \mathbf{u} = \mathbf{u}_h$  be the nodal interpolation of  $\mathbf{u}$  in finite element space  $\tilde{\mathbf{S}}_h^k$  and  $\mathbf{w}_h = \nabla \times \mathbf{u}_h$ . The finite element space  $\tilde{\mathbf{S}}_h^k$  is defined in (2.10), but it will be defined again in (3.7) next section with explicit nodal degrees of freedom (3.8). The nodal interpolation operator  $\mathbf{I}_h$  is defined by such nodal degrees of freedom (3.8). It is standard, cf. for example, [25], to show that  $\mathbf{I}_h$  interpolates smooth function  $\mathbf{u}$  in (2.4) in the optimal order of approximation, for  $r > 5/2$  in (2.4). We note that for less smooth functions,  $\mathbf{I}_h$  can be defined as an averaging interpolation operator such as the Scott–Zhang operator in [8, 20]. Then, by (2.14) and (2.4), we prove (2.13) as

$$\begin{aligned} \|\mathbf{B} - \mathbf{B}_h\|_{L^2(\Omega)^3} &\leq C_0^{-1} C_1 \|\mathbf{B} - \mathbf{w}_h\|_{L^2(\Omega)^3} = C_0^{-1} C_1 \|\nabla \times (\mathbf{u} - \mathbf{u}_h)\|_{L^2(\Omega)^3} \\ &= C_0^{-1} C_1 |\mathbf{u} - \mathbf{I}_h \mathbf{u}|_{\mathbf{H}(\text{curl})} \leq Ch^{\min\{k,r\}} \|\mathbf{u}\|_{H^{r+1}(\Omega)^3} \\ &\leq Ch^{\min\{k,r\}} \|\mathbf{B}\|_{H^r(\Omega)^3}. \end{aligned}$$

■

We remark that the  $\mathbf{u}$  above in the analysis is unique, but  $\mathbf{u}_h = \mathbf{I}_h \mathbf{u}$  may not be unique. That is, different  $\mathbf{I}_h$  can be used. Also  $\mathbf{u}_h$  may be defined by other ways than linear interpolation. What we need, in the analysis and in computation, is a unique, divergence-free

$$\mathbf{w}_h = \nabla \times \mathbf{u}_h.$$

Thus, this allows us to choose  $\mathbf{u}_h$  from a non divergence-free subspace  $\mathbf{S}_h^k$ , cf. (3.7), (3.17) and (3.16) below. Of course, in  $\mathbf{S}_h^k$   $\mathbf{u}_h$  is unique for  $\mathbf{w}_h$ , but not unique in  $\tilde{\mathbf{S}}_h^k$ . This is different from other computational methods where  $\mathbf{u}_h$  is also unique, divergence-free. We note that, with an appropriate boundary condition, a divergence-free and curl-free function in  $\tilde{\mathbf{S}}_h^k$  is  $\mathbf{0}$ .

### 3. 3D divergence-free basis

Let  $\Omega$  be the cube  $[0, 1]^3$  in 3D. The construction can be extended to domains which are a union of rectangular cubes, but not to general polyhedral domains. Let  $\mathcal{T}_h$  be an uniform grid of  $n^3$  cubes on  $\Omega$ , cf. Figures 4 and 5.

On the grid  $\mathcal{T}_h$ , the finite element space  $\mathbf{V}_h^k$  of (2.6) is simply the continuous Lagrange element. The number of nodal degrees of freedom in the  $x$ -direction, for the first component  $v_1$  of a  $\mathbf{V}_h^k$  function  $\mathbf{v}_h$ , on one element is  $(k+2)$ . With the continuity constraint and boundary condition  $\mathbf{n} \cdot \mathbf{v}_h = 0$ , the number of degrees of freedom is  $[(k+1)n - 1]$  in the  $x$ -direction. In the  $y$  and  $z$  directions, the first component is of polynomial degree  $k$ , and has no boundary condition, i.e.  $v_1(x, 0, 0)$ ,  $v_1(x, 1, 0)$ ,  $v_1(x, 0, 1)$ , and  $v_1(x, 1, 1)$  do not have to be *zero*. So the total degrees of freedom for  $v_1$  of  $\mathbf{v}_h \in \mathbf{V}_h^k$  is  $((k+1)n - 1)(kn + 1)^2$ . Hence the dimension is, for all three components,

$$\begin{aligned} \dim \mathbf{V}_h^k &= 3((k+1)n - 1)(kn + 1)^2 \\ &= 3k^3n^3 + 3k^2n^2 - 3kn + 3k^2n^3 + 6kn^2 + 3n - 3. \end{aligned} \quad (3.1)$$

In order to find the dimension of the divergence-free subspace of  $\mathbf{V}_h^k$ , we introduce the image space of divergence-operator:

$$P_h^k = \nabla \cdot \mathbf{V}_h^k = \left\{ \nabla \cdot \mathbf{v}_h \mid \mathbf{v}_h \in \mathbf{V}_h^k \right\} \subset Q_{k,k,k}^{-1,-1,-1}(\mathcal{T}_h). \quad (3.2)$$

Here we used a convenient notation so that  $Q_{k_1,k_2,k_3}^{\alpha_1,\alpha_2,\alpha_3}(\mathcal{T}_h)$  denotes the space of functions which has a continuous partial derivative of order  $\alpha_i$  in  $x_i$  direction and is piecewise polynomial of separated degrees  $k_i$  in  $x_i$  on the grid  $\mathcal{T}_h$ . For example,

$$Q_{k,k+1,k}^{0,1,0}(\Omega) = \left\{ v \in C^0(\Omega) \mid v_y \in C^0(\Omega), v|_K \in Q_{k,k+1,k}, \forall K \in \mathcal{T}_h \right\}.$$

By (3.2),  $P_h^k$  are discontinuous and piecewise  $Q_k$  polynomials on  $\mathcal{T}_h$ . The dimension of discontinuous  $Q_k$  functions,  $Q_{k,k,k}^{-1,-1,-1}(\mathcal{T}_h)$ , is  $(k+1)^3n^3$ . However, there are constraints on functions of  $P_h^k$  at so called singular vertices and singular edges of  $\mathcal{T}_h$ . The name singular vertex was introduced by Morgan and Scott in [15], cf. also [19, 24]. Here a singular vertex is a vertex where all planes meeting at the vertex fall into three crossing planes, cf. Figure 2.

We study the constraints on  $P_h^k$  functions. Let  $q_h \in P_h^k$  and  $\mathbf{v}_h = (v_1, v_2, v_3) \in \mathbf{V}_h^k$  be such that

$$q_h = \nabla \cdot \mathbf{v}_h = \partial_x v_1 + \partial_y v_2 + \partial_z v_3.$$

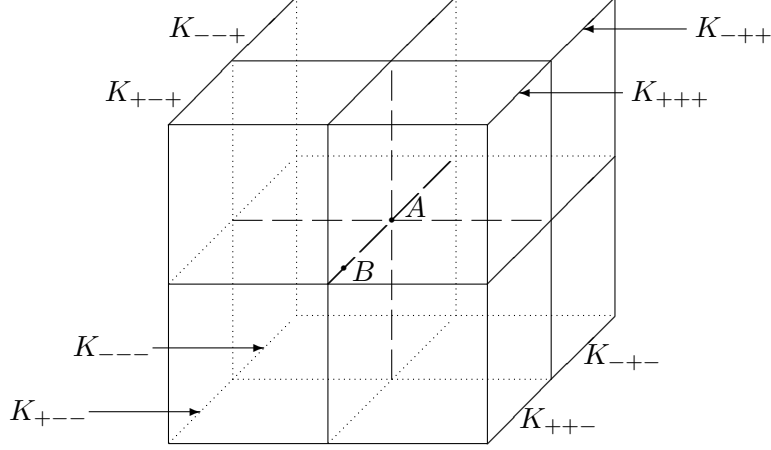


Figure 2: A singular vertex  $A$  and a node  $B$  on a singular edge, cf. (3.5) and (3.4).

Let node  $B$  be inside an edge, shared by four cubes,  $K_{+--}$ ,  $K_{+--}$ ,  $K_{+++}$ , and  $K_{+--}$ , cf. Figure 2. Due to the continuity of  $v_i$ , we have

$$\begin{cases} q_h|_{K_{+--}}(B) = \partial_x v_1|_{K_{+--}}(B) + \partial_y v_2|_{K_{+--}}(B) + \partial_z v_3|_{K_{+--}}(B), \\ q_h|_{K_{+--}}(B) = \partial_x v_1|_{K_{+--}}(B) + \partial_y v_2|_{K_{+--}}(B) + \partial_z v_3|_{K_{+--}}(B), \\ q_h|_{K_{+++}}(B) = \partial_x v_1|_{K_{+--}}(B) + \partial_y v_2|_{K_{+--}}(B) + \partial_z v_3|_{K_{+--}}(B), \\ q_h|_{K_{+--}}(B) = \partial_x v_1|_{K_{+--}}(B) + \partial_y v_2|_{K_{+--}}(B) + \partial_z v_3|_{K_{+--}}(B). \end{cases} \quad (3.3)$$

Therefore

$$q_h|_{K_{+--}}(B) - q_h|_{K_{+--}}(B) + q_h|_{K_{+++}}(B) - q_h|_{K_{+--}}(B) = 0. \quad (3.4)$$

That is,  $\{q_h(B)\}$  has three degrees of freedom, instead of four, when restricted on the four cubes meeting at  $B$ . At a singular vertex  $A$ , cf. **Figure 2**, we repeat the calculation (3.3)–(3.4) within the front four cubes, within the back four cubes, within the right four cubes, and within the top four cubes. It follows that

$$\begin{cases} q_h|_{K_{+--}}(A) - q_h|_{K_{+--}}(A) + q_h|_{K_{+++}}(A) - q_h|_{K_{+--}}(A) = 0, \\ q_h|_{K_{---}}(A) - q_h|_{K_{---}}(A) + q_h|_{K_{--+}}(A) - q_h|_{K_{--+}}(A) = 0, \\ q_h|_{K_{+++}}(A) - q_h|_{K_{+++}}(A) + q_h|_{K_{+--}}(A) - q_h|_{K_{+--}}(A) = 0, \\ q_h|_{K_{+++}}(A) - q_h|_{K_{+++}}(A) + q_h|_{K_{--+}}(A) - q_h|_{K_{--+}}(A) = 0. \end{cases} \quad (3.5)$$

By choosing  $v_i$  appropriately, we can show the three constraints in (3.5) are linearly independent. That is, the number of degrees of freedom of  $\{q_h(A)\}$  is precisely 4, instead of 8, when restricted on the 8 cubes. Let us give the details. There are 6 spanning functions  $v_i^\pm$ . For example,  $v_1^+$  is defined such that

$$\begin{aligned}\partial_x v_1^+|_{K_{+--}}(A) &= 1, \\ \partial_x v_1^+|_{K_{---}}(A) &= 0.\end{aligned}$$

Note that  $\{\partial_x v_1(A)\}$  has two degrees of freedom instead of 8. Let vector  $V_{q_h,A} = (q_h|_{K_{\pm\pm\pm}}(A))$  consist of the 8 values of  $\{q(A)\}$  on the 8 cubes. We have the following span, from the divergence of 6 spanning vectors.

$$\begin{aligned}\{V_{q_h,A}\} &= \text{span}\left\{\nabla \cdot \begin{pmatrix} v_1^+ \\ 0 \\ 0 \end{pmatrix}, \nabla \cdot \begin{pmatrix} v_1^- \\ 0 \\ 0 \end{pmatrix}, \nabla \cdot \begin{pmatrix} 0 \\ v_2^+ \\ 0 \end{pmatrix}, \right. \\ &\quad \left. \nabla \cdot \begin{pmatrix} 0 \\ v_2^- \\ 0 \end{pmatrix}, \nabla \cdot \begin{pmatrix} 0 \\ 0 \\ v_3^+ \end{pmatrix}, \nabla \cdot \begin{pmatrix} 0 \\ 0 \\ v_3^- \end{pmatrix}\right\}.\end{aligned}$$

That is,

$$\begin{aligned}\{V_{q_h,A}\} &= \text{span}\left\{\begin{pmatrix} 1 \\ 0 \\ 0 \\ 1 \\ 0 \\ 1 \\ 1 \\ 0 \end{pmatrix}, \begin{pmatrix} 0 \\ 1 \\ 1 \\ 0 \\ 1 \\ 0 \\ 0 \\ 1 \end{pmatrix}, \begin{pmatrix} 1 \\ 1 \\ 0 \\ 0 \\ 0 \\ 1 \\ 0 \\ 1 \end{pmatrix}, \begin{pmatrix} 0 \\ 0 \\ 1 \\ 1 \\ 0 \\ 0 \\ 0 \\ 0 \end{pmatrix}, \begin{pmatrix} 1 \\ 1 \\ 1 \\ 0 \\ 0 \\ 0 \\ 0 \\ 0 \end{pmatrix}, \begin{pmatrix} 0 \\ 0 \\ 0 \\ 1 \\ 1 \\ 1 \\ 1 \\ 1 \end{pmatrix}\right\} \\ &= \text{span}\left\{\begin{pmatrix} 1 \\ 0 \\ 0 \\ 1 \\ 0 \\ 1 \\ 1 \\ 0 \end{pmatrix}, \begin{pmatrix} 0 \\ 1 \\ 0 \\ 1 \\ 0 \\ 0 \\ 0 \\ 1 \end{pmatrix}, \begin{pmatrix} 1 \\ 1 \\ 0 \\ 0 \\ 0 \\ 1 \\ 0 \\ 1 \end{pmatrix}, \begin{pmatrix} 1 \\ 1 \\ 0 \\ 0 \\ 0 \\ 0 \\ 0 \\ 0 \end{pmatrix}\right\}.\end{aligned}$$

We list all constraints for a  $P_h^k$  function next.

1. For each internal vertex  $A$ ,  $q_h \in P_h^k$  has 8 nodal values when restricted on 8 elements sharing the vertex  $A$ . But there are constraints on these 8 values, cf. (3.5). We lose 4 degrees of freedom at each internal vertex for  $P_h^k$ . There are  $(n-1)^3$  internal vertices.
2. At each boundary vertex  $A$  which is interior to one face square of  $\partial\Omega$ , we have only 3 degrees of freedom for the functions in  $P_h^k$ , where the 4th degree of freedom is lost due to the 2D version singular vertex, similar to (3.4). There are 6 boundary faces and  $6(n-1)^2$  internal face-vertex.
3. On each internal edge, there are  $4(k-1)$  internal degrees of freedom for a  $Q_k$  function, when restricted on the 4 squares sharing the edge. Such an internal node ( $B$  in Figure 2) is also a 2D version singular vertex where  $P_h^k$  satisfies (3.4). There are edges in 3 directions and  $n(n-1)^2$  internal edges each direction.
4. Due to the boundary condition  $\mathbf{n} \cdot \mathbf{v}_h = 0$ , by the divergence theorem, the average of functions in  $P_h^k$  is zero, because  $\int_{\Omega} q_h d\mathbf{x} = \int_{\Omega} \nabla \cdot \mathbf{v}_h d\mathbf{x} = \int_{\partial\Omega} \mathbf{n} \cdot \mathbf{v}_h ds = 0$ . This gives one constraint.

Therefore, with these restrictions, we found the dimension

$$\begin{aligned} \dim P_h^k &= (k+1)^3 n^3 - 4(n-1)^3 \\ &\quad - 6(n-1)^2 - 3(k-1)n(n+1)^2 - 1. \end{aligned} \quad (3.6)$$

However, the counting above of constraints may not be complete, i.e., there might be additional constraints. To be complete, we need to find a  $\mathbf{V}_h^k$  function for each  $Q_{k,k,k}^{-1,-1,-1}(\mathcal{T}_h)$  satisfying the four points in the counting. This is what we did in 2D [24], in order to show the inf-sup condition. But here we omit this work, but only prove the dimension formula (3.6), in Proposition 3.1 below. Proposition 3.1 does ensure that the constraint counting above is correct and complete. Consequently, we find the dimension of the divergence-free subspace of  $\mathbf{V}_h^k$ , defined in (2.7),

$$\dim \mathbf{Z}_h^k = \dim \mathbf{V}_h^k - \dim P_h^k.$$

Next, we construct the potential spaces. By the conditions in defining  $\tilde{\mathbf{S}}_h^k$ , cf. (2.10), we give another definition to  $\tilde{\mathbf{S}}_h^k$ :

$$\begin{aligned} \tilde{\mathbf{S}}_h^k &= \left\{ \mathbf{s}_h = (s_1, s_2, s_3)^T \mid s_1 \in Q_{k,k+1,k+1}^{0,1,1}(\mathcal{T}_h), s_2 \in Q_{k+1,k,k+1}^{1,0,1}(\mathcal{T}_h), \right. \\ &\quad \left. s_3 \in Q_{k+1,k+1,k}^{1,1,0}(\mathcal{T}_h), \mathbf{n} \times \mathbf{s}_h = \mathbf{0} \right\}. \end{aligned} \quad (3.7)$$

By the method in [25], we can show the two definitions for  $\tilde{\mathbf{S}}_h^k$  are equivalent. But in analysis and in computation, we do not need this space  $\tilde{\mathbf{S}}_h^k$ . Instead, we need its subspace  $\mathbf{S}_h^k$ , defined in (2.11) and (3.17). We omit the analysis on  $\tilde{\mathbf{S}}_h^k$ . By [25], the nodal functionals defining  $Q_{k,k+1,k+1}^{0,1,1}$  on the reference element  $[0, 1]^3$  are

$$\begin{cases} f(\frac{i}{k}, \frac{j}{k-1}, \frac{l}{k-1}), & 0 \leq i \leq k, 0 \leq j, l \leq (k-1); \\ f_y(\frac{i}{k}, j, \frac{l}{k-1}), & 0 \leq i \leq k, 0 \leq j \leq 1, 0 \leq l \leq (k-1); \\ f_z(\frac{i}{k}, \frac{j}{k-1}, l), & 0 \leq i \leq k, 0 \leq j \leq (k-1), 0 \leq l \leq 1; \\ f_{yz}(\frac{i}{k}, j, l), & 0 \leq i \leq k, 0 \leq j, l \leq 1. \end{cases} \quad (3.8)$$

In particular, we plot the face degree-of-freedom at  $x = 0$  in Figure 3. By switching  $x$  and  $y$ , and  $x$  and  $z$ , the nodal functionals for the other two components of  $\tilde{\mathbf{S}}_h^k$  are defined similar to (3.8).

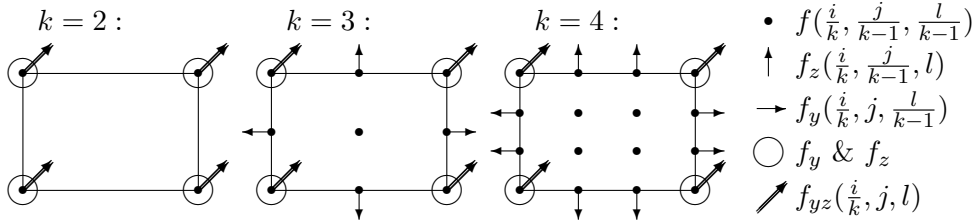


Figure 3: The face nodal values of  $Q_{k,k+1,k+1}^{0,1,1}$  at  $x = 0$ , cf. (3.8).

By (3.8) and the boundary condition  $\mathbf{n} \times \mathbf{s}_h = \mathbf{0}$ , we would get the dimension of  $\tilde{\mathbf{S}}_h^k$ :

$$\dim \tilde{\mathbf{S}}_h^k = 3(kn + 1)(kn)^2. \quad (3.9)$$

Though the dimension of  $\tilde{\mathbf{S}}_h^k$  is no less than that of  $\mathbf{Z}_h^k$ , it does not necessarily mean the image of  $\tilde{\mathbf{S}}_h^k$  would cover  $\mathbf{Z}_h^k$  under the curl operator. This is to be shown next, by finding a subspace of  $\tilde{\mathbf{S}}_h^k$  which has a kernel  $\{\mathbf{0}\}$  under the mapping of the curl operator.

Define two subspaces of  $\tilde{\mathbf{S}}_h^k$  by

$$\mathbf{S}_1 = \left\{ \mathbf{s} = (s_1 \ 0 \ 0)^T \mid \mathbf{s} \in \tilde{\mathbf{S}}_h^k \right\}, \quad (3.10)$$

$$\mathbf{S}_2 = \left\{ \mathbf{s} = (0 \ s_2 \ 0)^T \mid \mathbf{s} \in \tilde{\mathbf{S}}_h^k \right\}. \quad (3.11)$$

When studying the image space of  $\mathbf{S}_1 \oplus \mathbf{S}_2$  under the curl, we can see that the curl operator is a one-to-one mapping. Further, by checking the first

two components of  $\mathbf{V}_h^k$  and of  $\nabla \times (\mathbf{S}_1 \oplus \mathbf{S}_2)$ , the difference is an additional constraint on the image space, i.e.,

$$\int_0^1 \nabla \times \begin{pmatrix} s_1 \\ s_2 \\ 0 \end{pmatrix} (x_0, y_0, z) dz = \begin{pmatrix} 0 \\ 0 \\ c \end{pmatrix}, \quad \text{for all } 0 \leq x_0, y_0 \leq 1. \quad (3.12)$$

Here the constant  $c$  is the integral of the third component of  $\nabla \times (s_1, s_2, 0)$ , which may not be zero. Therefore  $\mathbf{S}_1$  and  $\mathbf{S}_2$  are not enough to span one space  $\mathbf{S}_h^k$ . We need some contribution of the third component of  $\tilde{\mathbf{S}}_h^k$ . To correct (3.12), we need only one degree of freedom for  $s_3$  in the  $z$  direction.

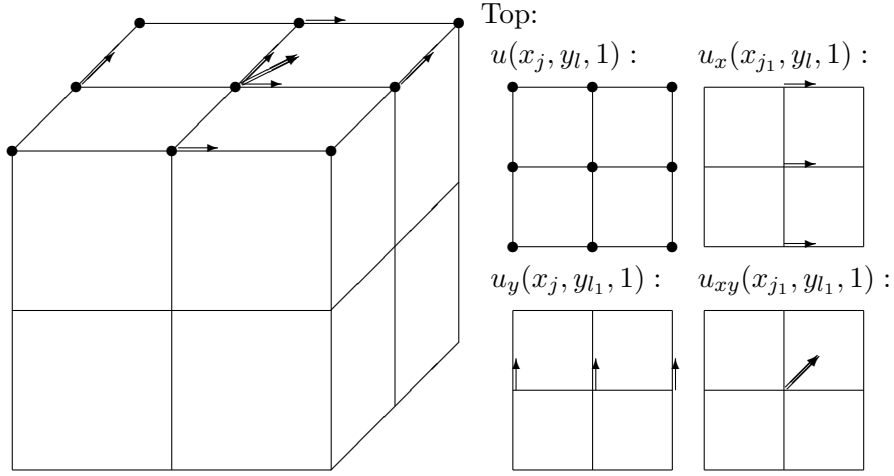


Figure 4: The linear functionals in  $F_T$  (3.14),  $k = 2$ ,  $n = 2$ .

Let the space  $\mathbf{S}_3$  be spanned by those nodal basis functions on the top face of  $\Omega$ ,  $\{(x, y, 1) \mid 0 \leq x, y \leq 1\}$ :

$$\mathbf{S}_3 = \left\{ \mathbf{s} = (0 \ 0 \ s_3)^T \mid \mathbf{s} \in \tilde{\mathbf{S}}_h^k, f_i(s_3) = 0 \text{ if } f_i \notin F_T \right\}, \quad (3.13)$$

where  $f_i$  stands for one nodal value functional defined in (3.8), and  $F_T$  is

defined by, cf. Figure 4,

$$\begin{aligned}
F_T = \{ & f_i \mid f_i(u) = u((n_1 + \frac{j}{k-1})h, (n_2 + \frac{l}{k-1})h, 1), \\
& u_x((n_1 + j_1)h, (n_2 + \frac{l}{k-1})h, 1), \\
& u_y((n_1 + \frac{j}{k-1})h, (n_2 + l_1)h, 1), \\
& u_{xy}((n_1 + j_1)h, (n_2 + l_1)h, 1), \\
& 0 \leq n_1, n_2 \leq (n-1), 0 \leq j, l \leq (k-1), 0 \leq j_1, l_1 \leq 1 \}. \quad (3.14)
\end{aligned}$$

We note that the boundary condition  $\mathbf{n} \times \mathbf{s}_3 = 0$  restricted  $\partial_x \mathbf{s}_3 = \partial_y \mathbf{s}_3 = \mathbf{0}$  on the boundary edges of top square  $z = 1$ , but  $\mathbf{s}_3 \neq 0$  there.

**Proposition 3.1.** *Let the spaces  $\mathbf{V}_h^k$  and  $\mathbf{Z}_h^k$  be defined by (2.6) and (2.7), respectively. Then*

$$\dim \mathbf{Z}_h^k = 2k^3n^3 + 3k^2n^2. \quad (3.15)$$

In addition,  $\dim \mathbf{S}_h^k = 2k^3n^3 + 3k^2n^2$  and

$$\nabla \times \mathbf{S}_h^k = \mathbf{Z}_h^k, \quad (3.16)$$

where

$$\mathbf{S}_h^k = \text{span}\{\mathbf{S}_1, \mathbf{S}_2, \mathbf{S}_3\}, \quad (3.17)$$

for  $\mathbf{S}_i$  defined in (3.10), (3.11) and (3.13).

**Proof .** By the definitions, we have that

$$\mathbf{S}_h^k \subset \tilde{\mathbf{S}}_h^k \quad \text{and} \quad \nabla \times \mathbf{S}_h^k \subset \mathbf{Z}_h^k.$$

First, the nodal basis functions in  $\mathbf{S}_1$  are linearly independent. For a non-zero  $\mathbf{s} \in \mathbf{S}_1$ , as long as it is non-zero at one node, its curl is non-zero. The same **reasoning** applies to  $\mathbf{S}_2$  and  $\mathbf{S}_3$ . Therefore

$$\dim \mathbf{S}_1 = \dim(\nabla \times \mathbf{S}_1) = (kn+1)(kn)^2, \quad (3.18)$$

$$\dim \mathbf{S}_2 = \dim(\nabla \times \mathbf{S}_2) = (kn+1)(kn)^2, \quad (3.19)$$

$$\dim \mathbf{S}_3 = \dim(\nabla \times \mathbf{S}_3) = (kn)^2. \quad (3.20)$$

Next, we show three functions in  $\nabla \times \mathbf{S}_1$ ,  $\nabla \times \mathbf{S}_2$  and  $\nabla \times \mathbf{S}_3$  are linearly independent. Let

$$c_1 \nabla \times \begin{pmatrix} s_1 \\ 0 \\ 0 \end{pmatrix} + c_2 \nabla \times \begin{pmatrix} 0 \\ s_2 \\ 0 \end{pmatrix} + c_3 \nabla \times \begin{pmatrix} 0 \\ 0 \\ s_3 \end{pmatrix} = \mathbf{0} \quad (3.21)$$

for some, not all zero,  $c_1, c_2$ , and  $c_3$ . If  $c_3 = 0$ , then the first two vectors are linearly dependent.  $\nabla \times (s_1, 0, 0)$  has its first component zero. This leads to  $c_2 = 0$  or  $\partial_z s_2 = 0$ . Because  $s_2(x, y, 0) = 0$ , by the boundary condition in (3.7),  $s_2 \equiv 0$ . Symmetrically,  $c_1 = 0$  or  $s_1 \equiv 0$ .

Let  $c_3 \neq 0$  in (3.21). From the first two components of the integral of (3.21) in  $z$  direction, by (3.12), we get

$$\int_0^1 \partial_y s_3 dz = 0, \quad \int_0^1 \partial_x s_3 dz = 0.$$

Thus

$$\int_0^1 s_3(x, y, z) dz = c_0$$

independent of  $x$  and  $y$ . Let  $x = y = 0$ . By the boundary condition for  $\mathbf{S}_3$ ,  $c_0 = 0$ . By the definition (3.13), the  $C^1$ - $P_k$ , 1D spline function  $s_3(x_0, y_0, z)$  has all nodal values 0 except at  $z = 1$ . By integrating the nodal basis function, one would get

$$\int_0^1 s_3(x_0, y_0, z) dz = C s_3(x_0, y_0, 1) = c_0 = 0, \quad (3.22)$$

for some nonzero  $C$  depending on  $k$  and  $n$ . Thus  $s_3(x, y, 1) \equiv 0$  for all  $x$  and  $y$ , by (3.22). Hence  $s_3 = 0$ . In (3.21), if a  $c_i \neq 0$ , then  $s_i = 0$ . The three vectors in (3.21) are **therefore** linearly independent.

Hence, for  $\mathbf{S}_h^k$  defined in (3.17), **we have by (3.18) that**

$$\begin{aligned} \dim\{\nabla \times \mathbf{s} \mid \mathbf{s} \in \mathbf{S}_h^k\} &= \dim \mathbf{S}_1 + \dim \mathbf{S}_2 + \dim \mathbf{S}_3 \\ &= (kn + 1)(kn)^2 + (kn + 1)(kn)^2 + (kn)^2 \\ &= 2k^3n^3 + 3k^2n^2. \end{aligned} \quad (3.23)$$

Since  $\{\nabla \times \mathbf{s} \mid \mathbf{s} \in \text{span}(\mathbf{S}_1, \mathbf{S}_2, \mathbf{S}_3)\} \subset \mathbf{Z}_h^k$ , **it follows from (3.23) that**

$$\dim \mathbf{Z}_h^k \geq 2k^3n^3 + 3k^2n^2. \quad (3.24)$$

On the other side, by counting singular vertices, we know that the dimension of  $P_h^k$  is no less than the number given in the right hand side of (3.6).

The dimension could be bigger if we missed any constraints in (3.6). However, by (3.1) and (3.6),

$$\begin{aligned} \dim \mathbf{Z}_h^k &= \dim \mathbf{V}_h^k - \dim P_h^k \\ &\leq [3k^3n^3 + 3k^2n^2 - 3kn + 3k^2n^3 + 6kn^2 + 3n - 3] \\ &\quad - [(k+1)^3n^3 - 4(n-1)^3 - 6(n-1)^2 - 3(k-1)n(n+1)^2 - 1] \\ &= 2k^3n^3 + 3k^2n^2. \end{aligned} \tag{3.25}$$

By comparing (3.24) and (3.25), (3.15) and (3.6) hold. Finally, by (3.23), the subspace  $\nabla \times \mathbf{S}_h^k$  is the same as the divergence-free space  $\mathbf{Z}_h^k$  as the dimension of the subspace is equal to that of the bigger space. ■

#### 4. Numerical tests

In this section, we report some numerical tests on solving (1.1) on the unit cube,  $\Omega = (0, 1)^3$ . The grids are obtained by the standard multigrid refinement, shown in Figure 5.

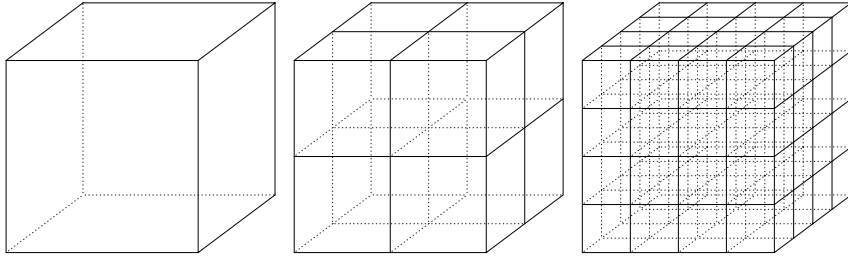


Figure 5: The first three levels of grids in the computations.

We choose the right hand side function  $\mathbf{J}$  for (1.1), with  $\mu(\mathbf{x}) = 1$  there, as

$$\mathbf{J} = \nabla \times \nabla \times \begin{pmatrix} g \\ g \\ 0 \end{pmatrix},$$

where

$$g = 2^{12}(x - x^2)^2(y - y^2)^2(z - z^2)^2.$$

The exact solution for the Maxwell equations (1.1) is

$$\mathbf{B} = \nabla \times \begin{pmatrix} g \\ g \\ 0 \end{pmatrix}. \quad (4.1)$$

In Table 1 we list the errors in  $L^2$ -norm for the finite element solutions of (2.8) and (4.1), for  $k = 2$ . Usually, we are interested in the  $L^2$  errors of  $\mathbf{B}$ , and the  $H^1$  errors for its vector potential, cf. for example, page 189 in Monk's book [13]. The number of conjugate-gradient iterations, used to solve the linear system of finite element equations up to the order of discretization error, is listed in the fifth column. Different from the typical finite element  $L^2$  equations, here the condition number for system (2.8) is not constant, but increases rapidly. This is because the basis functions for  $\mathbf{Z}_h^k$  in the computation (2.8) are not usual nodal basis, but the curl of nodal basis functions for  $\mathbf{S}_1$ ,  $\mathbf{S}_2$  and  $\mathbf{S}_3$ . In Table 1,  $\mathbf{B}_h^*$  is the solution when the CG stops at roughly the truncation error instead of the machine accuracy. If we continue the conjugate-gradient iteration to get an exact solution up to the computer accuracy, the number of conjugate-gradient iterations can exceed the number of unknowns in the linear system, see the last column in Table 1. This is not seen (by the authors) in solving other finite element equations by the CG method.

Table 1: The error and convergence rate for (4.1),  $k = 2$ .

level	$\dim \mathbf{Z}_h^k$	$\ \mathbf{B}^h - \mathbf{B}_h^*\ _{L^2}$	$h^n$	#CG	$\ \mathbf{B}^h - \mathbf{B}_h\ _{L^2}$	$h^n$	#CG
2	176	0.4283359		87	0.42833299		1118
3	1216	0.0620251	2.8	1051	0.06203413	2.8	10064
4	8960	0.0075215	3.0	2491	0.00752723	3.0	26531
5	68608	0.0008888	3.1	20178	0.00088926	3.1	44000

The order of convergence,  $n$ , in the fourth column of Table 1 is calculated by two consecutive errors. We note that the order of convergence for the computation in Table 1 is one higher than that proved in Theorem 2.2. This is commonly seen, a superconvergence phenomenon on uniform rectangular grids, cf. [22] for many general results. In fact, to display the superconvergence, we use a interpolated function

$$\mathbf{B}^h = \nabla \times \mathbf{I}_h \mathbf{J}$$

instead of  $\mathbf{B} = \nabla \times \mathbf{J}$ , in Tables 1, 2 and 3. Here  $\mathbf{I}_h \mathbf{J}$  denotes the nodal interpolation of  $\mathbf{J}$  in the space  $\tilde{\mathbf{S}}_h^k$ .

Next we compute (2.8) with the solution (4.1) again by the order  $k = 3$  finite element. The convergence is shown in Table 2, one order higher than the theory predicted. This is again a superconvergence on a uniform grid, which is not studied in this work. Again, the computer accuracy could be a problem that the CG iteration could take more than four times of the dimension. In theory, the CG assumes the exact solution at no more steps than the dimension, for a positive definite linear system.

Table 2: The convergence of  $\mathbf{Z}_h^k$ ,  $k = 3$ , for (2.8) with (4.1) .

level	$\dim \mathbf{Z}_h^k$	$\ \mathbf{B}^h - \mathbf{B}_h^*\ _{L^2}$	$h^n$	#CG	$\ \mathbf{B}^h - \mathbf{B}_h\ _{L^2}$	$h^n$	#CG
1	81	0.57247233		17	0.57977580		1267
2	540	0.03635564	4.0	123	0.03792754	3.9	13456
3	3888	0.00252970	3.8	2535	0.00253402	3.9	44881
4	29376	0.00016408	3.9	6446	0.00016394	4.0	79135

Finally, we numerically test another exact solution to the Maxwell equations (1.1), to be fair,

$$\mathbf{B} = \nabla \times \mathbf{J}, \quad \mathbf{J} = \begin{pmatrix} 0 \\ g \\ g \end{pmatrix}. \quad (4.2)$$

This is because our potential space  $\mathbf{S}_h^k = \mathbf{S}_1 \cup \mathbf{S}_2 \cup \mathbf{S}_3$  where  $\mathbf{S}_1$  and  $\mathbf{S}_2$  are full finite element spaces, cf. (3.10) and (3.11). So we intentionally choose a potential  $\mathbf{J} = (0, g, g)$  which cannot be approximated by our potential functions in  $\mathbf{S}_h^k$ . The error and convergence rate are listed in Table 3, for  $k = 3$  and  $k = 4$ . Comparing to the solutions to (4.1), reported in Table 2, there is no difference in convergence for (4.2), see the first four rows of Table 3.

When we solve the problem (1.1) with the solution (4.2) by  $k = 4$  finite element method, as the solution  $\mathbf{B}$  is inside the finite element space  $\mathbf{Z}_h^k$ , the finite element solution  $\mathbf{B}_h$  defined by (2.8) is exactly  $\mathbf{B}$ . This is shown in the last row of Table 3. The error would be zero if there is no computer round-off **error**, even on the first grid. We note again that the potential in  $\mathbf{S}_h^k$  for the solution  $\mathbf{B}_h$  is totally different from  $\mathbf{J}$ , but  $\mathbf{B}_h = \mathbf{B}$ . This is the advantage of the new method, not seeking the unique potential  $\mathbf{J}_h$  which is the divergence-free one.

**Acknowledgments.** The authors thank two anonymous referees who raised

Table 3: The error of the  $\mathbf{Z}_h^k$  solution to (4.2).

level	$\ \mathbf{B}^h - \mathbf{B}_h^*\ _{L^2}$	$h^n$	# CG	dim $\mathbf{Z}_h^k$
$k = 3$				
1	0.59058868261	0.0	29	81
2	0.03339096705	4.1	121	540
3	0.00232247484	3.8	4734	3888
4	0.00014621751	4.0	15801	29376
$k = 4$ ( $\mathbf{B} \in \mathbf{Z}_h^k$ )				
1	0.00000000201	0.0	594	176

many questions and made many constructive comments, **which greatly improve the manuscript.**

## References

- [1] C. Amrouche, C. Bernardi, M. Dauge, V. Girault, Vector potentials in three-dimensional non-smooth domains, *Math. Meth. Appl. Sci.* 21 (1998) 823–864.
- [2] R. Bensow, M. G. Larson, Discontinuous least squares finite element method for the div-curl problem, *Numer. Math.* 101 (2005) 601–617.
- [3] J. H. Bramble, J. E. Pasciak, A new approximation technique for div-curl systems, *Math. Comp.* 248 (2004) 1739–1762.
- [4] P. Ciarlet, *The Finite Element Method for Elliptic Problems*, North-Holland, Amsterdam, 1978.
- [5] B. Cockburn, F. Li, C.-W. Shu, Locally divergence-free discontinuous Galerkin methods for the Maxwell equations, *J. Comput. Phys.* 194 (2) (2004) 588–610.
- [6] F. Dubois, Discrete vector potential representation of a divergence free vector field in three dimensional domains: Numerical analysis of a model problem, *SIAM J. Numer. Anal.* 27 (1990) 1103–1142.
- [7] V. Girault, P. A. Raviart, *Finite Element Methods for the Navier-Stokes Equations, Theory and Algorithms*, Springer, Berlin, 1986.

- [8] V. Girault, L. R. Scott, Hermite interpolation of nonsmooth functions preserving boundary conditions, *Math. Comp.* 71 (239) (2002) 1043–1074.
- [9] V. Girault, L. R. Scott, A quasi-local interpolation operator preserving the discrete divergence, *Calcolo* 40 (2003) 1–19.
- [10] J. Huang, J. Zou, Uniform a priori estimates for elliptic and static maxwell interface problems, *Discrete and Cont. Dynam. Sys. Series B* 7 (2007) 145–170.
- [11] J. Jin, *The Finite Element Method in Electromagnetics*, Wiley, New York, 1993.
- [12] P. C. Jr., V. Girault, Condition inf-sup pour l'élément fini de Taylor–Hood P2-iso-P1, 3-D ; application aux équations de Maxwell, *C. R. Acad. Sci. Paris, Ser. I* 335 (2002) 827–832.
- [13] P. Monk, *Finite Element Methods for Maxwell's Equations*, Oxford University Press, Oxford, 2003.
- [14] P. Monk, S. Zhang, Multigrid computation of vector potentials, *J. Comp. Appl. Math.* 62 (1995) 301–320.
- [15] J. Morgan, L. R. Scott, A nodal basis for  $C^1$  piecewise polynomials of degree  $n \geq 5$ , *Math. Comp.* 29 (1997) 736–740.
- [16] J. Nédélec, Mixed finite elements in  $\mathbf{R}^3$ , *Numer. Math.* 35 (1980) 315–341.
- [17] R. A. Nicolaides, X. N. Wu, Covolume solutions of three-dimensional div-curl equations, *SIAM J. Numer. Anal.* 34 (1997) 2195–2203.
- [18] F. Rapetti, F. Dubois, A. Bossavit, Discrete vector potentials for non-simply connected three-dimensional domains, *SIAM J. Numer. Anal.* 41 (4) (2003) 1505–1527.
- [19] L. R. Scott, M. Vogelius, Norm estimates for a maximal right inverse of the divergence operator in spaces of piecewise polynomials, *RAIRO, Modelisation Math. Anal. Numer.* 19 (1985) 111–143.
- [20] L. R. Scott, S. Zhang, Finite-element interpolation of non-smooth functions satisfying boundary conditions, *Math. Comp.* 54 (1990) 483–493.

- [21] J. Stratton, *Electromagnetic Theory*, McGraw-Hill, New York, 1941.
- [22] L. Wahlbin, *Superconvergence in Galerkin Finite Element Methods*, vol. 1605 of *Lecture Notes in Mathematics*, Springer, Berlin, 1995.
- [23] X. Xu, S. Zhang, A new divergence-free interpolation operator with applications to the Darcy-Stokes-Brinkman equations, *SIAM J. Scientific Computing* 32 (2) (2010) 855–874.
- [24] S. Zhang, A family of  $Q_{k+1,k} \times Q_{k,k+1}$  divergence-free finite elements on rectangular grids, *SIAM J. Num. Anal.* 47 (2009) 2090–2107.
- [25] S. Zhang, On the full  $C_1$ - $Q_k$  finite element spaces on rectangles and cuboids, *Adv. Appl. Math. Mech.* 2 (2010) 701–721.